

Feasibility of small animal cranial irradiation with the microRT system

Erich L. Kiehl

Washington University School of Medicine, St. Louis, Missouri 63110

Strahinja Stojadinovic

Virginia Commonwealth University School of Medicine, Richmond, Virginia 23298

Kathleen T. Malinowski, David Limbrick, Sarah C. Jost, Joel R. Garbow, Joshua B. Rubin, Joseph O. Deasy, Divya Khullar, Enrique W. Izaguirre, Parag J. Parikh, and Daniel A. Low
Washington University School of Medicine, St. Louis, Missouri 63110

Andrew J. Hope

Princess Margaret Hospital, Toronto, Ontario M5G 2M9, Canada

(Received 19 June 2007; revised 12 August 2008; accepted for publication 13 August 2008; published 26 September 2008)

Purpose: To develop and validate methods for small-animal CNS radiotherapy using the microRT system. **Materials and Methods:** A custom head immobilizer was designed and built to integrate with a pre-existing microRT animal couch. The Delrin[®] couch-immobilizer assembly, compatible with multiple imaging modalities (CT, microCT, microMR, microPET, microSPECT, optical), was first imaged via CT in order to verify the safety and reproducibility of the immobilization method. Once verified, the subject animals were CT-scanned while positioned within the couch-immobilizer assembly for treatment planning purposes. The resultant images were then imported into CERR, an in-house-developed research treatment planning system, and registered to the microRTP treatment planning space using rigid registration. The targeted brain was then contoured and conformal radiotherapy plans were constructed for two separate studies: (1) a whole-brain irradiation comprised of two lateral beams at the 90° and 270° microRT treatment positions and (2) a hemispheric (left-brain) irradiation comprised of a single A-P vertex beam at the 0° microRT treatment position. During treatment, subject animals ($n=48$) were positioned to the CERR-generated treatment coordinates using the three-axis microRT motor positioning system and were irradiated using a clinical Ir-192 high-dose-rate remote after-loading system. The radiation treatment course consisted of 5 Gy fractions, 3 days per week. 90% of the subjects received a total dose of 30 Gy and 10% received a dose of 60 Gy. **Results:** Image analysis verified the safety and reproducibility of the immobilizer. CT scans generated from repeated reloading and repositioning of the same subject animal in the couch-immobilizer assembly were fused to a baseline CT. The resultant analysis revealed a 0.09 mm average, center-of-mass translocation and negligible volumetric error in the contoured, murine brain. The experimental use of the head immobilizer added ± 0.1 mm to microRT spatial uncertainty along each axis. Overall, the total spatial uncertainty for the prescribed treatments was ± 0.3 mm in all three axes, a 0.2 mm functional improvement over the original version of microRT. Subject tolerance was good, with minimal observed side effects and a low procedure-induced mortality rate. Throughput was high, with average treatment times of 7.72 and 3.13 min/animal for the whole-brain and hemispheric plans, respectively (dependent on source strength). **Conclusions:** The method described exhibits conformality more in line with the size differential between human and animal patients than provided by previous prevalent approaches. Using pretreatment imaging and microRT-specific treatment planning, our method can deliver an accurate, conformal dose distribution to the targeted murine brain (or a subregion of the brain) while minimizing excess dose to the surrounding tissue. Thus, preclinical animal studies assessing the radiotherapeutic response of both normal and malignant CNS tissue to complex dose distributions, which closer resemble human-type radiotherapy, are better enabled. The procedural and mechanistic framework for this method logically provides for future adaptation into other murine target organs or regions. © 2008 American Association of Physicists in Medicine. [DOI: [10.1118/1.2977762](https://doi.org/10.1118/1.2977762)]

Key words: brain, CNS, conformal radiotherapy, dose response, small-animal

I. INTRODUCTION

Animal models are an essential tool for the preclinical evaluation of novel oncological therapies. In an ideal world, these

models would allow for the recapitulation of human cancer treatments (combinations of chemotherapy, radiation therapy, and surgery) on a small-animal scale. However, animal oncological modeling has historically been limited by a lack of

small-scale, conformal radiotherapy.¹ Clinical conformal irradiators, while highly accurate and precise, are impractical for small-animal applications; smaller organs require smaller field sizes and more precise beam localization. To maintain conformality on a small-animal scale, error margins must be reduced by one order of magnitude to $\sim \pm 0.2$ mm.^{2,3} Given the dearth of animal-specific conformal radiotherapy systems and the intransitivity of clinical conformal irradiators to the animal arena, little progress has been made in animal-modeled, targeted radiotherapeutic response studies. While there has been progress in chemotherapeutic response experiments, the lack of an adequate radiotherapeutic analog has rendered the pursuit of combinatory cancer response studies exceedingly difficult.¹

Multiple studies involving murine brain irradiation have been reported, all of which utilized x-ray sources and functionally non-conformal approaches. Monje *et al.* delivered whole-brain irradiation to adult rats by applying a full-body field with selective body shielding, in an attempt to correct for the excessive field size.⁴ Mizumatsu *et al.* and Yuan *et al.* employed similar methods while irradiating multiple subjects simultaneously.^{5,6} In most cases, treatment-related toxicities were not reported, though Cotrim *et al.* noted a 60% decrease in salivary flow resulting from such an approach.⁷ In all the above studies, there is no reported dose distribution and no mention of dose homogeneity within the targeted brain.

Our group has developed and described a novel, small-animal conformal irradiator named microRT, following the standard naming convention used to distinguish between human and animal use. microRT integrates multi-modality imaging capabilities, a custom treatment planning system, and submillimeter accurate animal positioning and dose delivery. However, no reproducible, conformal microRT methods have been published to date. We now propose such a method for conformal radiotherapy targeting the murine brain, both in whole and in subregions. This novel method utilizes pretreatment CT imaging, custom head immobilization, and conformal radiotherapy planning to allow for the assessment of both normal and malignant tissue response in a prospective fashion. In this report, we investigate and report on the feasibility of using the microRT system in preclinical studies requiring murine brain irradiation. Components of the microRT system evaluated included the subject immobilization and target delineation accuracy; treatment planning, delivery, and throughput; and acute tolerability of the fractionated treatment regimens applied.

II. Methods and Materials

II.A. microRT

The components of the microRT system have been described previously.² In brief review, microRT utilizes: (1) a clinical, high-dose rate (HDR) remote after-loading system with a 3.6 mm length \times 0.65 mm diameter, cylindrical Ir-192 source (Nucletron, Columbia, Maryland); (2) a custom aluminum collimator assembly with tungsten collimator inserts (0.375 in. thickness \times 3.8 mm ID opening) at the 0°, 90°, 180°, and 270° treatment positions; (3) a translational three-axis motor assembly for couch positioning (Velmex, Bloomfield, New York); (4) a multi-axis stepper motor amplifier (Primatics, Tangent, Oregon); (5) a LABVIEW-based software interface to control the motor assembly; (6) a custom Delrin[®] animal couch with fiducial markers for CT registration; (7) a spatial digitizer for pretreatment couch-to-collimator calibration (Immersion, San Jose, California); (8) a DICOM-compliant custom treatment planning system, microRTP, based on a downloadable, in-house MATLAB-based software, CERR;⁸ and (9) a rapid dose calculation model, based on Monte Carlo simulations and a modified parametric beam model.²

II.B. Animal models

All animals were used in accordance with an established animal studies protocol approved by the Washington University School of Medicine Animal Studies Committee. We utilized multiple small-animal models for the multiple CNS studies performed using microRT. For tumor control and the evaluation of novel drugs in conjunction with radiotherapy, we utilized a well-described nude/nude mouse model (Jackson Laboratory, Bar Harbor, Maine) with intra-cranially implanted U87 tumor cells.⁹ For normal tissue studies, we utilized nude/nude and C57BL/6 mouse strains (Jackson Laboratory, Bar Harbor, Maine). In all cases, the care, feeding, and use of any drug or radiation therapy was defined by the specific animal studies protocol and the methods for each experiment. In most cases, the subject animals were in the 6–10 week age range during treatment. For imaging and reproducibility of setup experiments, we utilized animals across this range of ages in order to assess if animal size drastically impacted setup uncertainty.

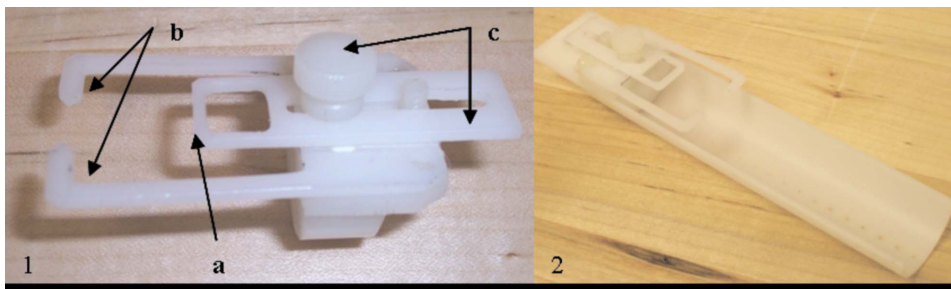


FIG. 1. (1) Custom head immobilization (HI) device showing (a) bite bar; (b) ear prongs; (c) slide adjustor and (2) microRT couch-HI assembly.

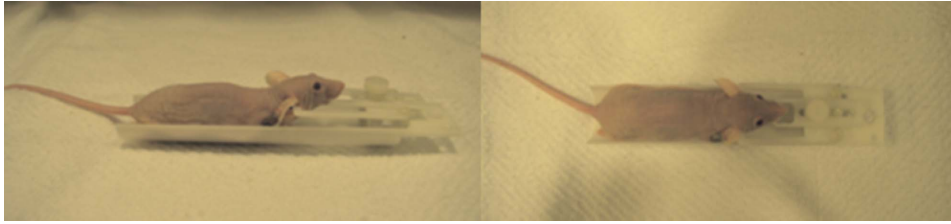


FIG. 2. Side/top views of subject animal positioned within the microRT couch-HI assembly, demonstrating the elevated head.

II.C. Anesthetization and immobilization

Prior to both imaging and irradiation, each subject animal was anesthetized via intra-peritoneal injection, using $5 \mu\text{l/g}$ mouse weight of a standard cocktail of 78.1% $d\text{H}_2\text{O}$, 19.0% ketamine (100 mg/mL), and 2.9% xylazine (100 mg/mL) by volume. Once full anesthesia was established, each subject was positioned within a custom, adjustable head immobilization (HI) device affixed to the microRT couch (Fig. 1). Immobilization was provided via three-point contact between (1) the HI device's bite bar and the animal's top teeth and (2–3) the HI device's prongs positioned within the animal's ear canals (Fig. 2).

II.D. Reproducibility of immobilization and contouring

Following anesthetization and positioning within the microRT couch-HI assembly, the same subject animal was CT-scanned using a Phillips Brilliance 16-slice Big Bore CT Scanner (Phillips Medical Systems; Bothell, WA) and was

then removed from the assembly, repositioned, and rescanned for a total of three scans. The resultant DICOM images were then imported into CERR using the custom "DICOM-import" CERR tool and were contoured (both brain and skin) using the custom CERR contouring tools.⁸ Then, using the "image fusion" tool in CERR, the three scans were fused using 6 degree of freedom rigid registration (resulting in couch assembly overlays) to an arbitrarily assigned base scan (one of the three aforementioned scans) registered in the custom microRTP treatment planning space. This registration was performed using CERR and a rigid registration algorithm, which generates a pure rotational and translational Euclidian transformation matrix with no scaling.⁸ Custom-written MATLAB analysis was subsequently performed on the fused scans to assess the translational and volumetric deformation errors resulting from subject repositioning within the immobilizer. Center-of-mass (COM), bounding box (3D-cube enclosing a structure), and volumetric values for the contoured brain were calculated and compared to those of the base

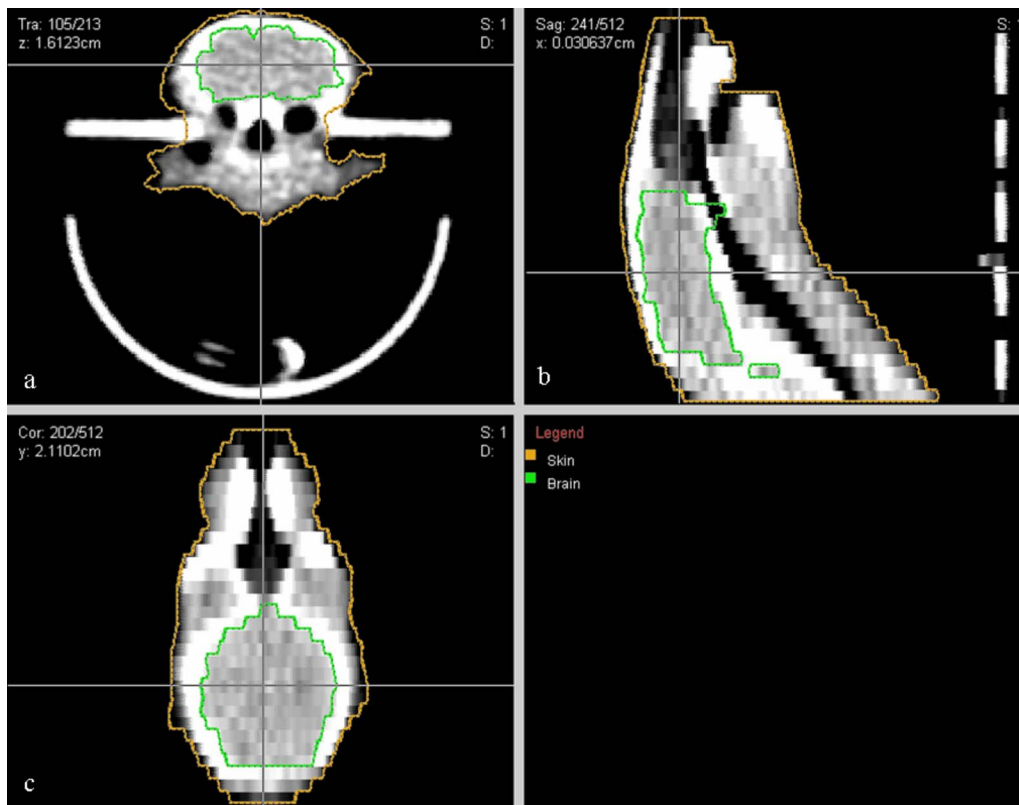


FIG. 3. CT image of a subject animal in microRT couch-HI assembly, contoured and registered in microRTP: (a) transverse view; (b) sagittal view; (c) coronal view.

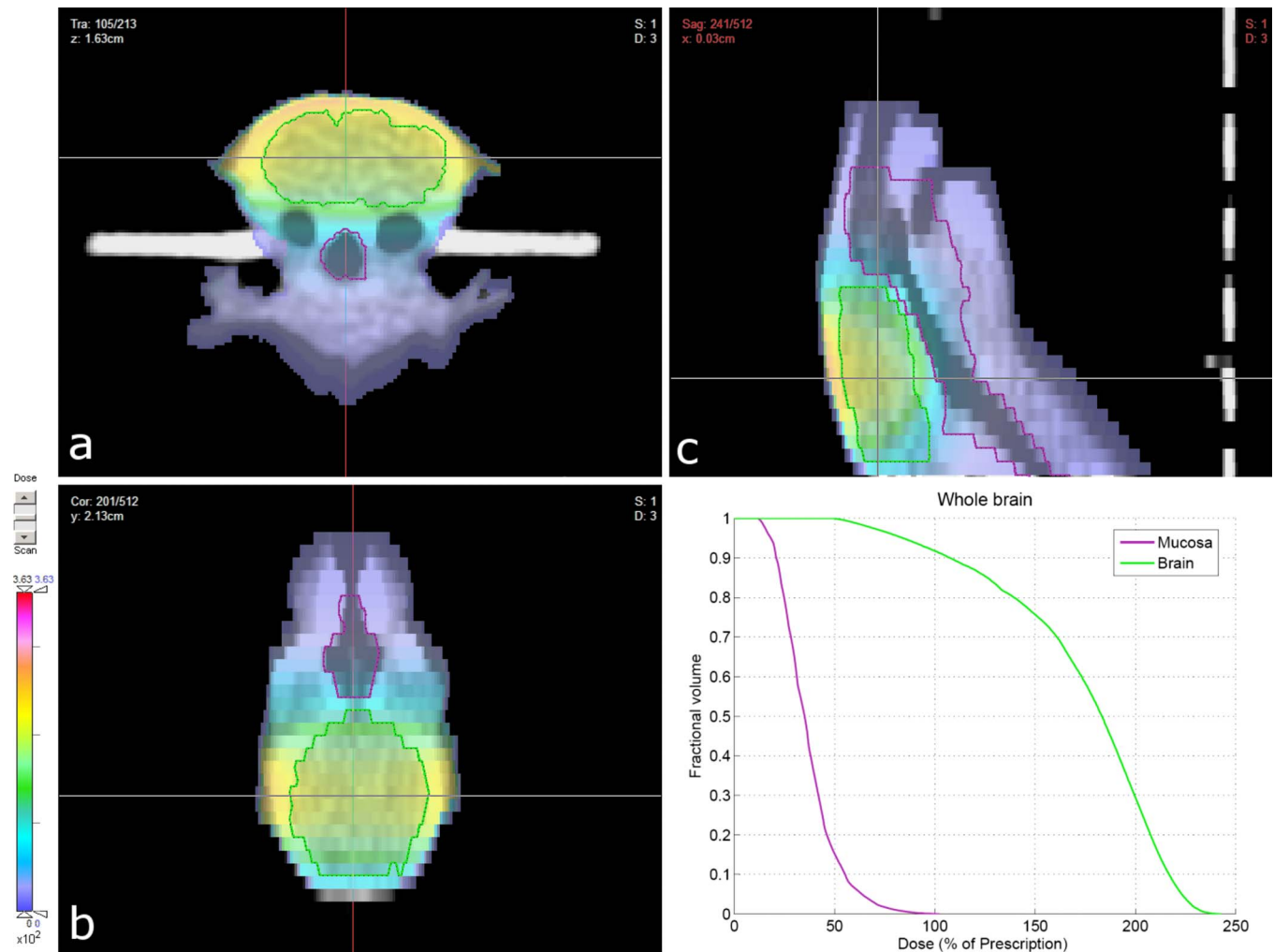


FIG. 4. Conformal radiotherapy plan and resultant dose distribution (summation of lateral beams) for whole-brain irradiation: (a) transverse view; (b) sagittal view; (c) coronal view. Dose units were set arbitrarily in the planning system and subsequently renormalized to the prescribed 5 Gy dose.

scan. In a similar manner, the brain structure from a single scan of the same subject animal was recontoured three times and analyzed to determine the amount of error attributable to human contouring inconsistencies.

II.E. Treatment planning

Under anesthesia, subject animals were positioned within the couch-immobilizer assembly and a CT scan was acquired, as described above. The CT images were imported into CERR, contoured, and registered in microRTP as above (Fig. 3). Conformal radiotherapy plans were then constructed for two separate CNS studies; one a whole-brain irradiation and one a hemispheric (left-brain) irradiation. Within the microRTP/microRT planning system, it is possible to vary the isocenter position, use one of four beam positions (current system), and vary the size of the tungsten collimators to generate different size beams. For both studies, the radiotherapy plans were designed to minimize exposure to the mucous membranes of the oral cavity, oropharynx, nasal structures, esophagus, trachea, eyes, and ears. For the whole-brain irradiation, the final treatment plan consisted of two

fields per fraction, utilizing equally weighted lateral beams (left and right) at the 90° and 270° microRT treatment positions (Fig. 4). For the hemispheric irradiation, the final treatment plan consisted of one field per fraction, utilizing an A-P vertex beam at the 0° microRT treatment position (Fig. 5). Dose-volume histograms were generated for each plan (Fig. 6). The 3D coordinates corresponding to the physical microRT treatment space for the constructed plans were then outputted in CERR for pre-treatment motor positioning.

II.F. Subject positioning

Before each treatment session, the microRT's three-axis motor positioning system was recalibrated to the physical coordinates of the microRT treatment space. In the original version of microRT, a spatial digitizer was used for the calibration procedure.² In these studies, the digitizer calibration was replaced by a LABVIEW-based program, which compared the rigid position of the microRT stage to the rigid positions of the limit switches on each of the three axes of the motor positioning system. Previously, the microRT positioning error during treatment was ± 0.5 mm, which was thought to be

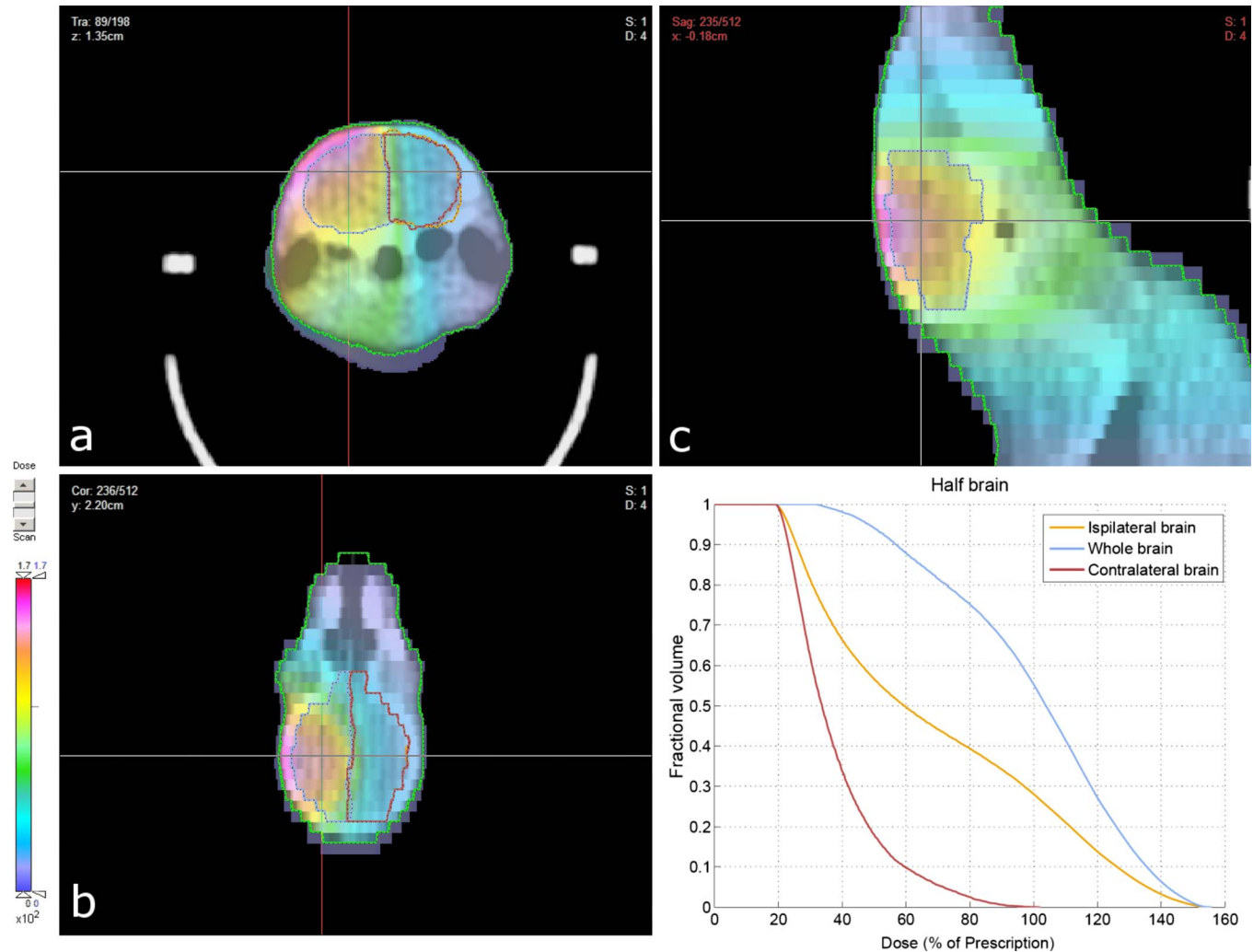


FIG. 5. Conformal radiotherapy plan and resultant dose distribution for hemispheric (left-brain) irradiation: (a) transverse view; (b) sagittal view; (c) coronal view. Dose units were not specified in the planning system and subsequently renormalized to the prescribed 5 Gy dose.

due to the ± 0.3 mm error of the spatial digitizer.² Using the mechanical switch-to-stage calibration, that source of error has been eliminated. Once microRT had been properly calibrated and anesthesia and immobilization had been administered, the subject in couch was loaded onto the microRT stage and positioned to the CERR-outputted coordinates using the software interface.



FIG. 6. Immobilized subject animal positioned within the microRT collimator assembly at the 90° and 270° microRT treatment positions, respectively, for whole-brain irradiation.

II.G. Irradiation

For the whole-brain irradiation, each animal ($n=38$) was treated with two lateral beams at the 90° and 270° microRT treatment positions, 2.5 Gy per beam, prescribed to midline, for a total of 5 Gy per fraction per animal (Fig. 6). Each animal received six fractions for a total dose of 30 Gy. For the hemispheric irradiation, each animal ($n=10$) was treated with one vertex beam at the 0° microRT treatment position, prescribed to midline, for a total of 5 Gy per fraction per animal (Fig. 7). Half of the animals in this study received six fractions for a total dose of 30 Gy, while the other half received 12 fractions for a total dose of 60 Gy. For the 30 and 60 Gy dose levels, fractions were delivered 3 days/week (Monday, Wednesday, Saturday) over two- and four-week periods, respectively. The animals were treated according to the generated radiotherapy plans using a clinical Ir-192 HDR remote after-loading system (Nucletron, Columbia, Maryland) collimated via the microRT collimator system. Given the inputted couch coordinates and the targeted fraction dose, treatment times were calculated using the modified paramet-

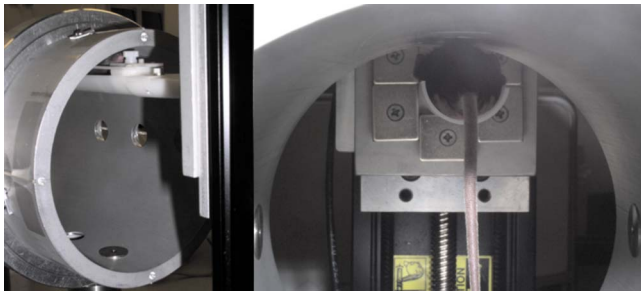


FIG. 7. Front/rear views of an immobilized subject animal positioned within the microRT collimator assembly at the 0° microRT treatment position for hemispheric (left-brain) irradiation.

ric beam and dose models previously described by Stojadinovic *et al.*² The delivered dose rate averaged ~ 90 cGy/min over the treatment course.

III. RESULTS

III.A. Immobilization and contouring accuracy

The fused 3-CT scan set and the 3 \times -recontoured CT scan used to assess immobilization and contouring reproducibility can be found in Figs. 8 and 9, respectively. By visual inspection, the two figures exhibit a relatively equivalent (low) level of contour variation, indicating that a substantial amount of immobilization reproducibility error may be explained by contouring inconsistencies. A more quantitative

TABLE I. Average translational and volumetric deformation errors from Fig. 8 analysis of brain contours (3-CT fused scans).

Translocation error	x	y	z
Bounding box (mm)	0.08	0.34	1.53
Center of mass (mm)	0.07	0.16	0.17
Volumetric error			
Volume (mm ³)	6.30		

comparison, resulting from the aforementioned MATLAB analysis, can be derived from Tables I and II. For the fused scans across all axes (Fig. 8), the Matlab analysis revealed the following averages: COM deviation of 0.12 mm, bounding box deviation of 0.65 mm, and volumetric deviation of 6.30 mm³. Similarly, for the recontoured scan (Fig. 9), COM deviation was 0.04 mm, bounding box deviation was 0.52 mm, and volumetric deviation was 3.56 mm³. Bounding box deviation proved rather ineffective as an error gauge, due to its sensitivity to singular stray contours. Conversely, volume differences were observed to be small in both cases. When adjusted for contouring inconsistencies, the fused images recorded a small 2.74 mm³ average volume difference, roughly equivalent to a 1% change in brain volume (from an average volume of 270 mm³). The most quantitatively significant finding was an average adjusted COM translocation of 0.09 mm across all axes. The use of the HI device effec-

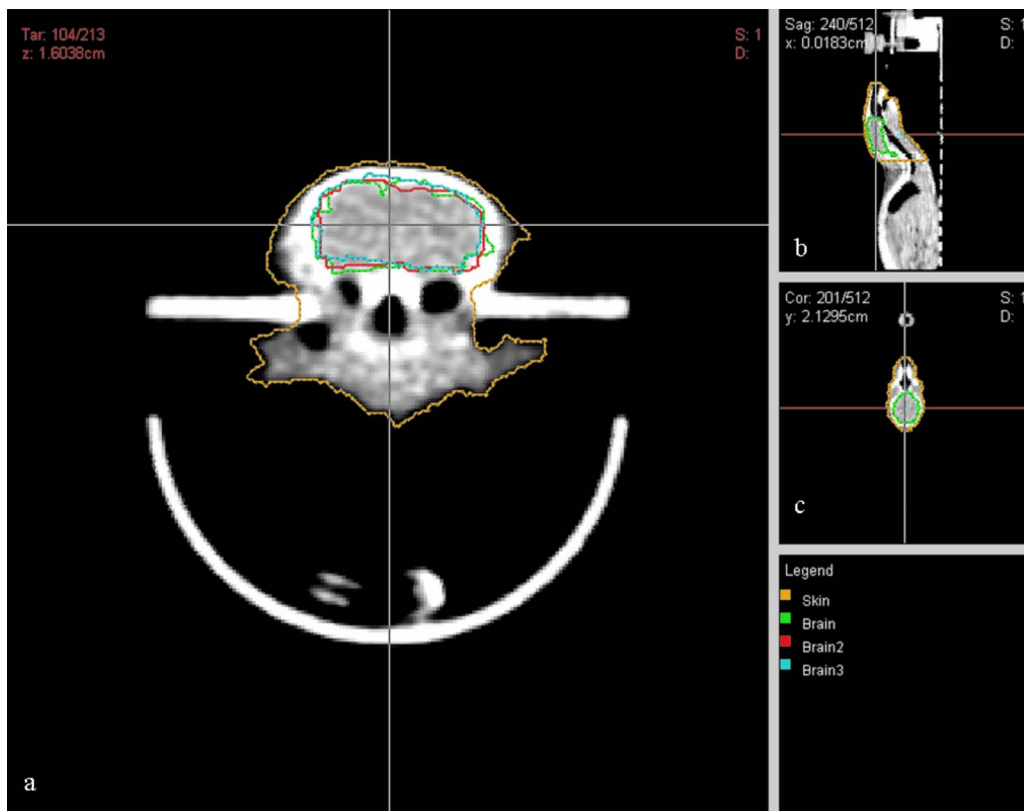


FIG. 8. Translationally and rotationally fused CT scans of the same subject animal re-positioned and rescanned three times in the microRT couch-HI assembly: (a) transverse view; (b) sagittal view; (c) coronal view.

TABLE II. Average translational and volumetric deformation errors from Fig. 9 analysis of brain contours ($3\times$ recontoured CT scan).

Translocation error	x	y	z
Bounding box (mm)	0.19	1.31	0.05
Center of mass (mm)	0.01	0.01	0.10
Volumetric error			
Volume (mm^3)	3.56		

tively added an additional ± 0.1 mm to the existing microRT margins.

III.B. Treatment throughput

The pretreatment setup, which includes couch-to-collimator calibration and the loading of treatment plan data into both the source and microRT software interfaces, initially took ~ 30 min to complete. By the last fraction, setup time had been optimized to ~ 15 min. Over the course of the fractionated treatment period, the air-kerma strength of the Ir-192 source ranged from 1.705 to 3.010 $\text{cGy m}^2/\text{h}$. Consequently, the treatment times varied in turn; a summary can be found in Table III. In total, the treatment times per 5 Gy fraction/animal averaged 7.72 min for the whole-brain plan and 3.13 min for the hemispheric plan. The lower average treatment time per unit dose delivered for the hemispheric irradiation was due to the setup geometry, which allowed for

a shorter source-to-target distance at the 0° treatment position. Repositioning times between opposed lateral beams and between subject animals decreased by half to ~ 30 s at the completion of the studies. Conversely, the time required to remove and store this system remained relatively constant throughout at ~ 10 min. Postoptimization, a cage of five mice treated with a 5 Gy fraction required an average of 68.1 min and 42.7 min for the whole-brain and hemispheric irradiations, respectively.

III.C. Subject outcomes

No complications were observed related to either the HI's bite bar or its ear prongs positioned within the subject's ear canals (Fig. 3). Both prescribed radiotherapy plans (Figs. 4 and 5) provided adequate avoidance of the tissues that were to be avoided, although the whole-brain plan was slightly more conformal in this regard. The hemispheric plan did display slightly elevated dose levels (~ 2.2 Gy, 44% of max dose) near the esophagus and trachea (Fig. 5). Overall, both regimens were tolerated well. Minimal skin erythema was observed and the subject animals were not in distress, dehydrated, or suffering from mucositis. Of the 48 total animals irradiated in both studies combined, 43 survived the entire treatment course (90%) with three mortalities attributed to anesthesia, resulting in a procedure-induced mortality rate of 6.3%.



FIG. 9. The brain structure from one CT scan of the same subject animal from Fig. 8 contoured three times to measure the relative amount of error attributable to human contouring inconsistencies: (1) transverse view; (2) sagittal view; (3) coronal view.

TABLE III. Summary of irradiation times for whole-brain and hemispheric irradiations.

Irradiation time	Per beam			Per fraction		
	Min (s)	Max (s)	Avg. (s)	Min (s)	Max (s)	Avg. (s)
<i>Whole-brain</i>	181.4 (3.02 min)	281.5 (4.69 min)	231.5 (3.86 min)	362.8 (6.05 min)	563.0 (9.62 min)	462.9 (7.72 min)
<i>Hemispheric</i>	141.3 (2.36 min)	234.4 (3.91 min)	187.9 (3.13 min)	141.3 (2.36 min)	234.4 (3.91 min)	187.9 (3.13 min)

IV. DISCUSSION

Using the described procedures, we have developed and characterized a conformal method of murine CNS radiotherapy. Our novel method is the first standardized approach that utilizes microRT to deliver conformal irradiation to an immobilized, small-animal target organ or region. Improvements in microRT error margins resulted in radiotherapy with increased conformal character, which was administered in an efficient manner well-tolerated by its animal subjects. With a targeted region of the murine brain, this method can be employed (and adapted) to conduct a myriad of preclinical studies assessing the radiotherapeutic response of both normal and malignant brain tissue with or without additional treatments (chemotherapy, surgery, etc.).

Unlike previous methods of small-animal brain irradiation, our technique is more conformal and provides 3D dose distribution information as well as dose-volume data. Prior preclinical brain irradiations have been predominated by nonuniform, nontargeted dose delivery resulting from full-body radiation fields with selective shielding.⁴⁻⁷ Utilizing pretreatment imaging and custom treatment planning, our method delivers targeted, uniformized radiation to the murine brain and its substituent regions. The surrounding tissue is effectively spared from excess dose, without the use of body shielding.

As opposed to clinical conformal devices, which carry average treatment uncertainty of ± 2 mm², microRT provides accuracy to within ± 0.2 mm in all translational axes, covering a wide range of potential treatment areas, including the murine brain. This level of accuracy represents a 0.3 mm improvement over the original version of microRT due to improvements in the calibration procedure and elimination of the spatial digitizer error. Previously, microRT possessed maximum spatial errors of ± 0.5 mm, more accurate than human conformal irradiators by a factor of 4, yet still shy of the targeted factor of 10 for true, small-animal conformality.² The improved ± 0.2 mm spatial uncertainty is more in line with the relative size differential between human and animal subjects.

Additionally, the microRT system integrates many modern clinical radiotherapy features, including 3D dose distribution analysis, custom immobilization, image guidance, multi-beam treatment planning, and computer-controlled positioning. Our method utilized a custom immobilization device in combination with the existing microRT hardware for the first time. CT imaging and the subsequent MATLAB analysis validated the safety and reproducibility of the novel HI

device and revealed a minimal, $\sim \pm 0.1$ mm increase in overall microRT treatment margins (to ± 0.3 mm) when utilizing the head immobilization system. The multi-modality imaging compliance of the couch-HI assembly (Delrin[®] composition for both) and the slide adjustability of the HI's bite bar further allowed for the pretreatment imaging and conformal treatment planning of subject animals of a variety of ages and sizes. We constructed and deployed two such conformal plans in separate studies, a multi-beam, whole-brain irradiation and a single-beam, hemispheric irradiation. However, given the availability of four microRT beam orientations, our method would allow for the similar construction and deployment of additional, multi-beam, conformal plans including sub-total irradiations (e.g., quarter-brain) and more complex dose distributions.

For the administered treatment plans, the radiation regimen was tolerated well with minimal side effects, a low treatment-related mortality rate (6.3%), and relatively high average animal throughput. This reflects well on the future feasibility of similar, large-scale studies delivering conformal radiation using microRT (to the murine brain and elsewhere), though future systems may utilize gas anesthetics in an attempt to reduce the rate of anesthetic-related mortality. The combination of ± 0.3 -mm-accurate radiation, custom immobilization, multi-modality pretreatment imaging, conformal radiotherapy planning, and high subject tolerance and throughput in this study effectively renders this first targeted microRT method the most efficacious and efficient small-animal model of clinical, conformal CNS radiotherapy to date. The comprehensive, conformal nature of microRT provides the fundamental framework to improve radiation therapy studies on tumor kinetics and therapeutic response and to pursue combinatory cancer studies including conformal radiotherapy approaches. Our method would be easily adaptable to conformal radiotherapy of other murine target regions via the creation and integration of additional immobilization devices and alternate conformal treatment plans.

Multiple areas for improvement do still exist within the microRT and microRTP frameworks. Although the improved error margins for microRT satisfy the targeted order of magnitude accuracy increase compared to human conformal devices, the inclusion of HI elevates the overall treatment margins, albeit slightly, above the targeted ± 0.2 mm threshold. Additionally, the previously verified accuracy of microRT dose delivery to within 10% of the prescribed dose (using radiochromic film measurements)² still exceeds the clinically accepted 5% error level. It has also occasionally proved dif-

difficult to provide the desired level of dose uniformity throughout the targeted tissue in the microRTP system (Fig. 5). Thus, while the described microRT method is currently the most conformal approach on a small-animal scale, it remains shy of true conformality. Further fundamental microRT accuracy and uniformity improvements should and will be pursued.

The inclusion of additional, bracketed treatment positions beyond the current four would allow for the creation of more complex multi-beam radiotherapy plans and, hence, more complex and uniformized dose distributions. One potential solution that has been both researched and proposed is a hardware conversion to an kV x-ray radiation source featuring a rotational immobilization system and a static gantry.¹⁰ Such a system could provide both translational and rotational conformal functionality and may potentially increase the set of deliverable radiotherapy plans. With respect to methods improvements, throughput could potentially be further increased through the integration of a shielded, multi-subject loading device with gas anesthesia. Such a device should decrease intra-plan and inter-animal repositioning lag times and is currently in the prototyping phase awaiting testing. Additionally, while the current couch and head immobilization are compatible with CT and microCT, microMR, microPET, microSPECT, and optical imaging modalities, the current microRTP couch registration process has only been tested using CT. The revision of the CERR software to allow for registration with all compatible imaging modalities would increase the functional use of a wider variety of imaging options and would create a system of co-registration; this research is currently ongoing. Lastly, experimentation in methods expansion into other immobilized murine target regions will be pursued.

V. CONCLUSIONS

The method described exhibits conformality more in line with the size differential between human and animal patients than provided by previous prevalent approaches. Using pre-treatment imaging and microRT-specific treatment planning, our method can deliver an accurate, conformal dose distribution to the targeted murine brain (or a subregion of the brain) while minimizing excess dose to the surrounding tissue.

Thus, preclinical animal studies assessing the radiotherapeutic response of both normal and malignant CNS tissue to complex dose distributions, which closer resemble human-type radiotherapy, are better enabled. The procedural and mechanistic framework for this method logically provides for future adaptation into other murine target organs or regions. Multiple studies of murine CNS response to radiation therapy delivered using the microRT system are ongoing.

ACKNOWLEDGMENTS

This work supported in part by NIH R21CA108677 and Varian Medical Systems.

- ¹S. Stojadinovic, D. A. Low, M. Vivic, S. Mutic, J. O. Deasy, A. J. Hope, P. J. Parikh, and P. W. Grigsby, "Progress toward a microradiation therapy small animal conformal irradiator," *Med. Phys.* **33**, 3834–3845 (2006).
- ²S. Stojadinovic, D. A. Low, A. J. Hope, M. Vivic, J. O. Deasy, J. Cui, D. Khullar, P. J. Parikh, K. T. Malinowski, E. W. Izaguirre, S. Mutic, and P. W. Grigsby, "MicroRT-small animal conformal irradiator," *Med. Phys.* **34**, 4706–4716 (2007).
- ³C. DesRosiers, M. S. Mendonca, C. Tyree, V. Moskvina, M. Bank, L. Massaro, R. M. Bigsby, A. Caperall-Grant, S. Valluri, J. R. Dynlacht, and R. Timmerman, "Use of the Leksell Gamma Knife for localized small field lens irradiation in rodents," *Technol. Cancer Res. Treat.* **2**, 449–454 (2003).
- ⁴M. L. Monje, H. Toda, and T. D. Palmer, "Inflammatory blockade restores adult hippocampal neurogenesis," *Science* **302**, 1760–1765 (2003).
- ⁵H. Yuan, M. W. Gaber, K. Boyd, C. M. Wilson, M. F. Kiani, and T. E. Merchant, "Effects of fractionated radiation on the brain vasculature in a murine model: blood-brain barrier permeability, astrocyte proliferation, and ultrastructural changes," *Int. J. Radiat. Oncol., Biol., Phys.* **66**, 860–866 (2006).
- ⁶S. Mizumatsu, M. L. Monje, D. R. Morhardt, R. Rola, T. D. Palmer, and J. R. Fike, "Extreme sensitivity of adult neurogenesis to low doses of X-irradiation," *Cancer Res.* **63**, 4021–4027 (2003).
- ⁷A. P. Cotrim, A. L. Sowers, B. M. Lodde, J. M. Vitolo, A. Kingman, A. Russo, J. B. Mitchell, and B. J. Baum, "Kinetics of tempol for prevention of xerostomia following head and neck irradiation in a mouse model," *Clin. Cancer Res.* **11**, 7564–7568 (2005).
- ⁸J. O. Deasy, A. I. Blanco, and V. H. Clark, "CERR: a computational environment for radiotherapy research," *Med. Phys.* **30**, 979–985 (2003).
- ⁹Y. Sun, N. O. Schmidt, K. Schmidt, S. Doshi, J. B. Rubin, R. V. Mulkern, R. Carroll, M. Ziu, K. Erkmen, T. Y. Poussaint, P. Black, M. Albert, D. Burstein, and M. W. Kieran, "Perfusion MRI of U87 brain tumors in a mouse model," *Magn. Reson. Med.* **51**, 893–899 (2004).
- ¹⁰A. J. Hope, S. Stojadinovic, J. O. Deasy, J. Hubenschmidt, P. W. Grigsby, and D. A. Low, "TH-C-230A-08: A prototype rotational immobilization system for a proposed static-gantry microRT device with tomographic capabilities," *Med. Phys.* **33**, 2272 (2006), abstract.